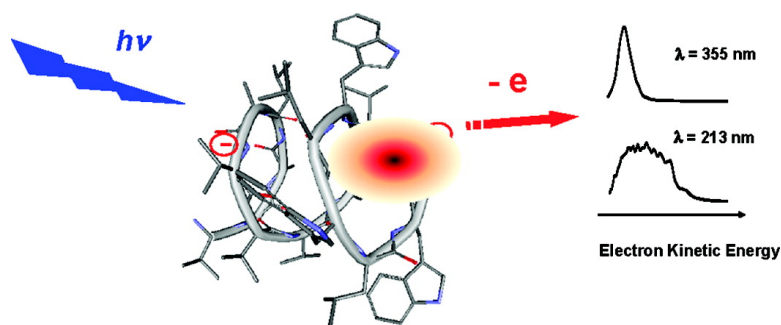


Photoelectron Spectroscopy of Gramicidin Polyanions: Competition between Delayed and Direct Emission

Katerina Matheis, Laure Joly, Rodolphe Antoine, Franck Lepine, Christian Bordas,
 Oli T. Ehrler, Abdul-Rahman Allouche, Manfred M. Kappes, and Philippe Dugourd

J. Am. Chem. Soc., **2008**, 130 (47), 15903-15906 • DOI: 10.1021/ja803758w • Publication Date (Web): 31 October 2008

Downloaded from <http://pubs.acs.org> on February 8, 2009



More About This Article

Additional resources and features associated with this article are available within the HTML version:

- Supporting Information
- Access to high resolution figures
- Links to articles and content related to this article
- Copyright permission to reproduce figures and/or text from this article

[View the Full Text HTML](#)

Photoelectron Spectroscopy of Gramicidin Polyanions: Competition between Delayed and Direct Emission

Katerina Matheis,[†] Laure Joly,[‡] Rodolphe Antoine,[‡] Franck Lépine,[‡] Christian Bordas,[‡] Oli T. Ehrler,[†] Abdul-Rahman Allouche,[‡] Manfred M. Kappes,^{*,†} and Philippe Dugourd^{*,‡}

Institut für Physikalische Chemie, Universität Karlsruhe, Kaiserstrasse 12, D-76128 Karlsruhe, Germany, and Université de Lyon, F-69622 Lyon, France; Université Lyon 1, Villeurbanne; CNRS, UMR 5579, LASIM

Received May 20, 2008; E-mail: manfred.kappes@chemie.uni-karlsruhe.de; dugourd@lasim.univ-lyon1.fr

Abstract: We present the first photoelectron (PE) spectra of polypeptide polyanions. Combining PE spectroscopy and mass spectrometry provides a direct measurement of the stability of the polyanions with respect to electron detachment and of the repulsive energy between excess charges. The second electron affinity of gramicidin was found to amount to 2.35 ± 0.15 eV, and the value of the repulsive Coulomb barrier was estimated to be 0.5 ± 0.15 eV. The spectra are interpreted as resulting from a competition between delayed and direct emission.

1. Introduction

While historically mass spectrometric and more recently spectroscopic studies of peptides have mostly involved positive ions, there is a growing analytical interest in acidic peptides that result from post-translational modifications, i.e., phosphorylation, sulfation, or glycan-bearing sialic acid. These peptides can benefit from examination in the negative mode.¹ Novel ion–electron,² ion–ion,³ and photo⁴ fragmentation techniques for polyanions have emerged. All of these techniques involve radical species that are obtained after electron loss from the precursor ion and fragmentation that is directed by the radical position. Beyond the analytical interest, these experiments raise a number of fundamental questions concerning the electronic structures of the precursor ions and the electron-detachment mechanisms. The possibility of undergoing electron loss after excitation, in addition to unimolecular decay via ionic fragmentation, is certainly the most exotic property of polyanions.^{5,6} An important concept to have emerged is that of novel potential energy surfaces describing the interaction of a single electron with the anionic molecular host. This gives rise to Coulomb barriers due to the strong repulsive energy between the negative

excess charges.^{7,8} Electron detachment can then occur through electron tunneling from metastable ground or excited electronic states.⁹ For a floppy system like a polypeptide, the large number of degrees of freedom adds to the complexity. Charges are present at remote locations, and the repulsive energy depends on the conformation. Moreover, it has been shown in atomic clusters^{10,11} that the combination of a high density of vibrational states together with strong rovibronic couplings and a low electron binding energy is particularly favorable for the development of delayed electron emission. Therefore, because of their low electron affinities, polypeptide polyanions are expected to exhibit substantial delayed detachment after energy redistribution induced by nonadiabatic couplings.

In this work, we present the first photoelectron (PE) spectra recorded on polypeptide polyanions. Experiments were performed on gramicidin, which is a biosynthetic product from *Bacillus brevis* that derives its functionality from the formation of a monovalent cation-selective channel in the lipid bilayer of targeted cells.¹² Gramicidin was chosen because of the presence of four tryptophan residues, leading to strong UV absorption and efficient electron emission. Recently, gas-phase infrared and UV spectra were reported for this peptide.^{13,14} Combining PE spectroscopy and mass spectrometry provides a direct measure-

[†] Universität Karlsruhe.

[‡] Université de Lyon.

- (1) Bowie, J. H.; Brinkworth, C. S.; Dua, S. *Mass Spectrom. Rev.* **2002**, *21*, 87–107.
- (2) Kjeldsen, F.; Silivra, O. A.; Ivonin, I. A.; Haselmann, K. F.; Gorshkov, M.; Zubarev, R. A. *Chem.—Eur. J.* **2005**, *11*, 1803–1812.
- (3) Coon, J. J.; Shabanowitz, J.; Hunt, D. F.; Syka, J. E. P. *J. Am. Soc. Mass Spectrom.* **2005**, *16*, 880–882.
- (4) (a) Gabelica, V.; Tabarin, T.; Antoine, R.; Rosu, F.; Compagnon, I.; Broyer, M.; De Pauw, E.; Dugourd, P. *Anal. Chem.* **2006**, *78*, 6564–6572. (b) Antoine, R.; Joly, L.; Tabarin, T.; Broyer, M.; Dugourd, P.; Lemoine, J. *Rapid Commun. Mass Spectrom.* **2007**, *21*, 265–268.
- (5) (a) Weber, J. M.; Ioffe, I. N.; Berndt, K. M.; Löffler, D.; Friedrich, J.; Ehrler, O. T.; Danell, A. S.; Parks, J. H.; Kappes, M. M. *J. Am. Chem. Soc.* **2004**, *126*, 8585–8589. (b) Wang, X.-B.; Wang, L.-S. *Nature* **1999**, *400*, 245–248.
- (6) Wang, L.-S.; Wang, X.-B. *J. Phys. Chem. A* **2000**, *104*, 1978–1990.

- (7) Simons, J.; Skurski, P.; Barrios, R. *J. Am. Chem. Soc.* **2000**, *122*, 11893–11899.
- (8) Boxford, W. E.; Dessent, C. E. H. *Phys. Chem. Chem. Phys.* **2006**, *8*, 5151–5165.
- (9) (a) Wang, X. B.; Ding, C. F.; Wang, L. S. *Chem. Phys. Lett.* **1999**, *307*, 391–396. (b) Ehrler, O. T.; Yang, J.-P.; Sugiharto, A. B.; Unterreiner, A. N.; Kappes, M. M. *J. Chem. Phys.* **2007**, *127*, 184301.
- (10) (a) Lépine, F.; Bordas, C. *Phys. Rev. A* **2004**, *69*, 053201. (b) Campbell, E. E. B.; Levine, R. D. *Annu. Rev. Phys. Chem.* **2000**, *51*, 65–98.
- (11) (a) Andersen, J. U.; Bonderup, E.; Hansen, K. J. *Chem. Phys.* **2001**, *114*, 6518–6525. (b) Andersen, J. U.; Bonderup, E.; Hansen, K. J. *Phys. B: At., Mol. Opt. Phys.* **2002**, *35*, R1–R30.
- (12) (a) Langs, D. A. *Science* **1988**, *241*, 188–191. (b) Burkhart, B. M.; Gassman, R. M.; Langs, D. A.; Pangborn, W. A.; Duax, W. L. *Biophys. J.* **1998**, *75*, 2135–2146.

ment of the stability of the polyanions with respect to electron detachment and of the repulsive energy between excess charges.

2. Experimental Section

Sample Preparation. Gramicidin from *B. brevis* was dissolved at a concentration of 250 μM in 20/80 (v/v) $\text{H}_2\text{O}/\text{MeOH}$ + 0.1 M KOH and directly electrosprayed. The gramicidin A variant ($\text{HCO}-\text{ValGlyAlaLeuAlaValValValTrpLeuTrpLeuTrpLeuTrp}-\text{N}-\text{HCH}_2\text{CH}_2\text{OH}$) was selected in the mass spectrum and used for all of the experiments.

Photoelectron Spectroscopy. The experimental setup is described in detail in ref 15. Briefly, ions were accumulated for $1/30$ s in a hexapole ion trap. These ions were then mass-separated using a reflectron time-of-flight (TOF) mass spectrometer. After mass selection, the ions were impulsively decelerated and then entered the detachment zone of a “magnetic bottle” type of TOF PE spectrometer, where they interacted with the third, fourth, or fifth harmonic of a pulsed Nd:YAG laser (with a pulse duration of 5–6 ns and typical fluences of 30, 15, and 1 mJ/cm^2 at photon energies of 3.49, 4.66, and 5.83 eV, respectively). The typical kinetic energy resolution achieved in our spectrometer was $\Delta E_{\text{kin}}/E_{\text{kin}} < 5\%$ at $E_{\text{kin}} = 1$ eV. The spectra were calibrated against the known photoelectron spectrum of I^- .

Electron Photodetachment Yield Measurements. The experimental setup^{14,16} consisted of a quadrupole ion-trap mass spectrometer (ThermoFinnigan, San Jose, CA, with a mass range of 50–2000 and mass resolution of 6500) coupled to an OPO laser pumped by a 355 nm Nd:YAG laser (with a pulse width of 5 ns and a 20 Hz repetition rate). Frequency doubling allowed scanning in the 215–330 nm range. The ions were injected into the trap, mass-selected, and then laser-irradiated inside the ion trap. Mass spectra were systematically recorded as a function of the laser wavelength. The photodetachment yield is equal to $\ln[(\text{parent} + \text{fragment})/\text{parent}]/(\lambda P_L)$, where λ is the laser wavelength and P_L is the laser power.

Solution Spectra. UV–vis spectra in solution were recorded using an AvaSpec-2048 fiber-optic spectrometer, an AvaLight-DH-S deuterium halogen light source, and a UV–vis cuvette by Avantes.

3. Results and Discussion

PE spectra of the doubly deprotonated dianion of the gramicidin A variant ($[\text{M} - 2\text{H}]^{2-}$) are shown in Figure 1. When plotted in the electron binding energy (EBE) domain, the spectra obtained at photon energies of 3.49 and 4.66 eV show a broad peak at $\text{EBE} = 2.82$ and 4.04 eV, respectively. At a photon energy of 5.83 eV, a series of reproducible features superimposed on a broad band is observed. Linear extrapolation of the low-binding-energy slopes onto the binding energy axis yields an estimated second electron affinity of 2.35 ± 0.15 eV.

First, we want to discuss the broad bands observed in Figure 1. As opposed to the tails at low binding energy, the positions of these broad structures are not common in the three spectra. They can hardly be connected to a given transition in the system. The situation becomes clearer if the spectra are plotted versus electron kinetic energy (EKE) instead of EBE (Figure 2). The most striking consequence of this alternative plot is that the broad features observed at photon energies of 3.49 and 4.66

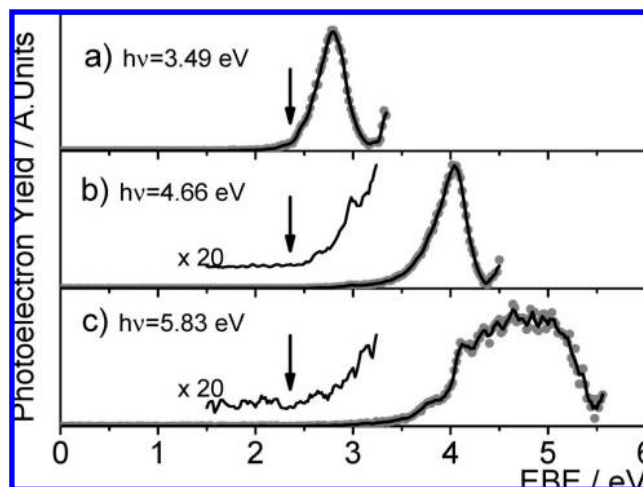


Figure 1. PE spectra of $[\text{M} - 2\text{H}]^{2-}$ at photon energies of 3.49, 4.66, and 5.83 eV ($\text{EBE} = h\nu - \text{EKE}$). The arrows mark the estimated value of the detachment energy. The gray dots are raw data points, and the solid line is a five-point-averaged curve to guide the eye.

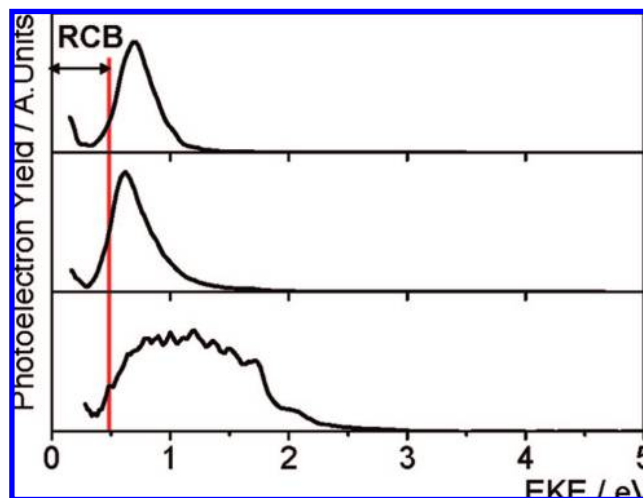


Figure 2. Kinetic energy spectra of $[\text{M} - 2\text{H}]^{2-}$ measured at photon energies of (top to bottom) 3.49, 4.66, and 5.83 eV. The red vertical line shows the value of the repulsive Coulomb barrier (RCB).

eV now appear at roughly the same position in the two spectra, independent of the photon energy. While this has not yet been measured for polyanions, the shape of the bands with a decreasing exponential tail on the high-EKE side and the observation of the band at the same EKE for different photon energies strongly suggest the observation of delayed emission.¹⁰ The cutoff in the low-EKE part of the spectrum is used to extract the repulsive Coulomb barrier (RCB) value, which was found to be 0.5 ± 0.15 eV. Using an ion trap coupled to a tunable laser,¹⁶ we also recorded the total detachment yield as a function of the laser wavelength between 210 and 330 nm. The wavelength-dependent electron yield is found to coincide with the absorption spectrum, which is consistent with resonant photoexcitation (of the UV chromophore Trp) as the critical step inducing electron loss (see Figure 3).^{17,18} Delayed emission may occur after resonant photoexcitation either from a long-

(13) Abo-Riziq, A.; Crews, B. O.; Callahan, M. P.; Grace, L.; de Vries, M. S. *Angew. Chem., Int. Ed.* **2006**, *45*, 5166–5169.

(14) Joly, L.; Antoine, R.; Broyer, M.; Lemoine, J.; Dugourd, P. *J. Phys. Chem. A* **2008**, *112*, 898–903.

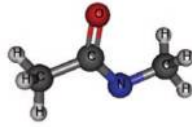
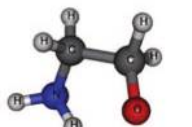
(15) Arnold, K.; Balaban, T. S.; Blom, M. N.; Ehrler, O. T.; Gilb, S.; Hampe, O.; van Lier, J. E.; Weber, J. M.; Kappes, M. M. *J. Phys. Chem. A* **2003**, *107*, 794–803.

(16) Talbot, F. O.; Tabarin, T.; Antoine, R.; Broyer, M.; Dugourd, P. *J. Chem. Phys.* **2005**, *122*, 074310.

(17) Kordel, M.; Schooss, D.; Gilb, S.; Blom, M. N.; Hampe, O.; Kappes, M. M. *J. Phys. Chem. A* **2004**, *108*, 4830–4837.

(18) Joly, L.; Antoine, R.; Allouche, A.-R.; Broyer, M.; Lemoine, J.; Dugourd, P. *J. Am. Chem. Soc.* **2007**, *129*, 8428–8429.

Table 1. Vertical Detachment Energy (VDE) and Adiabatic Detachment Energy (ADE) of the Anionic $\text{CH}_3\text{CONCH}_3$ and Ethanolamine Molecules^a

Molecule and deprotonated structure	B3LYP	MP2
 N-methylacetamide	VDE (eV)	2.81
	ADE (eV)	2.48
 2-aminoethanol	VDE (eV)	2.15
	ADE (eV)	1.90

^a Calculations were performed at the B3LYP/aug-cc-pvdz and MP2/aug-cc-pvdz levels of theory. All of the geometries were optimized at the B3LYP/aug-cc-pvdz level. The MP2/aug-cc-pvdz energies were calculated using the B3LYP/aug-cc-pvdz-optimized geometries.

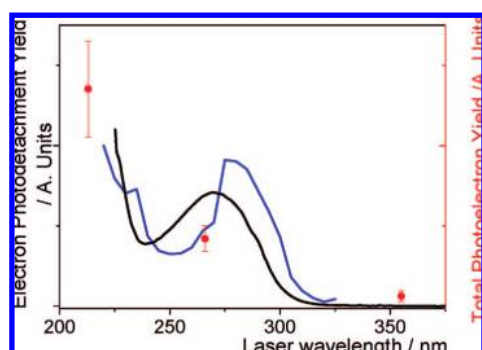


Figure 3. Electron photodetachment yield spectrum measured in the ion trap (blue curve) compared to the total photoelectron yields for the isolated $[\text{M} - 2\text{H}]^{2-}$ gramicidin ions obtained using the time-of-flight PE spectrometer at 213, 266, and 355 nm (red circles). The black curve shows the normalized absorption spectrum of gramicidin in solution.

lived excited state that couples to the ionization continuum via electron-tunneling emission⁹ or after internal conversion leading to emission from the ground state.^{10,11} In the latter case, energy redistribution among a subset of the vibrational degrees of freedom of the molecule would lead to a strong local increase in temperature followed by the electron detachment.

At 5.83 eV (Figure 2, bottom panel), the shape of the broad band and the features superimposed upon it show that delayed emission is not the only mechanism responsible for electron emission. At such a high photon energy, a dense manifold of excited states of the monoanion becomes accessible (corresponding to remaining $\pi-\pi^*$ excitations), increasing the direct detachment cross section. A very similar mixed spectrum composed of direct and delayed electrons has been observed in the case of negatively charged carbon clusters.¹⁹ In this latter case, the interpretation relies on the competition between direct photodetachment and thermionic emission, which can be clearly disentangled using time-resolved imaging spectrometry.

We now discuss the experimental EBE and RCB values that have been deduced from Figures 1 and 2. Gramicidin A has one acidic alcohol function at the C terminus. We can localize one negative charge on this site. Potential sites for further

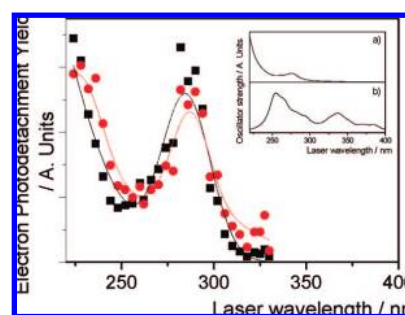


Figure 4. Electron photodetachment yields measured as a function of the laser wavelength for $[\text{M} - 2\text{H}]^{2-}$ (black squares) and $[\text{M} - 3\text{H}]^{3-}$ (red circles). Inset: TDDFT-calculated absorption spectra for (a) tryptophan and (b) tryptophan deprotonated on the nitrogen atom. The B3LYP functional and aug-cc-pvdz basis set were used for the calculations (40 states were included in each calculation).

deprotonation are on nitrogen atoms of either the tryptophan residues or the backbone amide functions. To discriminate between these two possibilities, we recorded UV action spectra of $[\text{M} - 2\text{H}]^{2-}$ and $[\text{M} - 3\text{H}]^{3-}$. The main fragments observed in the corresponding mass spectra after UV excitation are the oxidized species $[\text{M} - 2\text{H}]^{2-\bullet}$ and $[\text{M} - 3\text{H}]^{2-\bullet}$ resulting from the loss of one electron. The electron detachment yields are shown in Figure 4. A large band centered at $\lambda = 290$ nm is observed in both spectra. It is due to indole $\pi-\pi^*$ excitation. The position of this band shows that the indole ring in tryptophan is not deprotonated. Deprotonation of the indole would have induced a bathochromic shift, as recently observed for tyrosine-containing peptides¹⁸ and as predicted by time-dependent density functional theory (TDDFT) calculations (see the Figure 4 inset). Therefore, the second deprotonation must occur on the backbone. To estimate the electron detachment energies for the different sites theoretically, we calculated the vertical detachment energy (VDE) and adiabatic detachment energy (ADE) for each of two small molecular mimics: $\text{CH}_3\text{CONCH}_3$ and ethanolamine $\text{NH}_2\text{CH}_2\text{CH}_2\text{O}$ (Table 1). The geometries for the two molecules (anionic and neutral) were optimized at the B3LYP/aug-cc-pvdz level of calculation.²⁰ At this level of theory, the calculated electron affinities of the

(19) Wills, J. B.; Pagliarulo, F.; Baguenard, B.; Lépine, F.; Bordas, C. *Chem. Phys. Lett.* **2004**, *390*, 145–150.

(20) (a) Becke, A. D. *J. Chem. Phys.* **1993**, *98*, 5648–5652. (b) Lee, C.; Yang, W.; Parr, R. G. *Phys. Rev. B* **1988**, *37*, 785–789. (c) Dunning,

isolated deprotonated amide and ethanolamine functions are 2.48 and 1.90 eV, respectively. However, it is known that although B3LYP optimizations generally give accurate geometries, this method is not as reliable in ordering energies.²¹ For this reason, we computed the energies using MP2/aug-cc-pvdz²² single-point calculations on the B3LYP-optimized geometries. We obtained ADE values of 2.67 and 2.11 eV, respectively, for the two molecules, in good agreement with the B3LYP results. To compare the calculated EBE values to the experimental detachment energies, one has to take into account the influence on the EBE of the second charge, which has two effects: it reduces the EBE and leads to the formation of the RCB. While the RCB and the Coulomb shift do not necessarily coincide, the two effects have the same order of magnitude.^{6,7} The calculated binding energy values should thus be compared to 2.85 eV (EBE + RCB). This favors the observations of electrons emitted mainly from a deprotonated amide of the peptide backbone, whose calculated ADE and VDE values bracket the experimental value. The estimated RCB value (0.5 eV) corresponds to a distance r between the two charges of ~ 14.4 Å (using $\text{RCB} = e^2/\epsilon r$ with $\epsilon = 2$). The distance between the first backbone nitrogen and the C-terminus alcohol function obtained for the α -helical gramicidin is 12.6 Å.²³ This suggests that the structure

of $[\text{M} - 2\text{H}]^{2-}$ is more elongated in the gas phase than in solution. A possible structure would be a helix with a partial unfolding of the ends induced by the repulsion between the two charges. Partial unfolding due to repulsion between multiple charges has, for example, already been observed for multiply deprotonated oligonucleotides.²⁴

4. Conclusion

In this work, we have reported the first PE spectra measured on gas-phase polypeptides. We have shown that delayed emission is a competitive process to direct detachment in polypeptides. The balance between these different processes needs to be explored, and time-resolved experiments would help us gain deeper insight into the electron-emission dynamics. Binding and RCB energies have been determined. This gives quantitative data for comparison with calculations on electron loss and related processes and can provide crucial information for the development of new methods for structural analysis of negatively charged peptides. The RCB value measured here is in agreement with a relatively extended structure. The measurement of RCB, in particular for acidic peptides where deprotonation sites are well-localized, appears to be a novel and promising technique for obtaining structural information on gas-phase polypeptides.

JA803758W

T. H., Jr. *J. Chem. Phys.* **1989**, *90*, 1007–1023. (d) Kendall, R. A., Jr.; Harrison, R. J. *J. Chem. Phys.* **1992**, *96*, 6796–6806.

(21) Grimme, S. *J. Phys. Chem. A* **2005**, *109*, 3067–3077.

(22) (a) Hehre, W. J.; Radom, L.; Schleyer, P. v. R.; Pople, J. A. *Ab Initio Molecular Orbital Theory*; Wiley: New York, 1986. (b) Bartlett, R. H.; Stanton, J. F. *Rev. Comput. Chem.* **1994**, *5*, 65–169.

(23) Townsley, L. E.; Tucker, W. A.; Sham, S.; Hinton, J. F. *Biochemistry* **2001**, *40*, 11676–11686.

(24) Hoaglund, C. S.; Liu, Y.; Ellington, A. D.; Pagel, M.; Clemmer, D. E. *J. Am. Chem. Soc.* **1997**, *119*, 9051–9052.